Recent Trends in Sturctural Integrity Assessment, Eds.: V.R. Ranganath, S. Tarafder, A. Bahadur, 18-19 January 2001, National Metallurgical Laboratory, Jamshedpur, India, pp.105-129.

Fracture Mechanisms and the Quantification of Fracture Resistance

S. TARAFDER

National Metallurgical Laboratory, Jamshedpur 831 007

ABSTRACT

While structural components may fail and cease to fulfil their functions due to a variety of reasons, failure through fracture, due to the formation and growth of cracks, remain one of the most common methods of loss of structural integrity. It is therefore necessary to understand the process of fracture and be able to quantify the resistance of materials to it. An attempt has been made in this paper to present an overview of fracture mechanisms and fracture mechanics based tests. The process of fatigue crack growth, brittle cleavage fracture, ductile fracture through microvoid coalescence, and intergranular fracture has been reviewed. The philosophy and procedures of standard fracture toughness and fatigue crack growth tests have been discussed.

INTRODUCTION

The assurance of integrity of a structure essentially entails the statement of confidence that the structure can and will continue to fulfil the purpose for which it is made. Intended purposes can vary widely, and a structure may fail to meet the requirements of its function due to a variety of reasons. For example:

1. a slender load-bearing column may collapse due to instability initiated by elastic buckling
2. a watch spring may fail to keep proper timing due to excessive elastic deformation
3. a cantilever beam may bend under an overload due to plastic deformation
4. the walls of boiler tubes may thin down due to plastic deformation through creep
5. a rotating shaft may break into two pieces due to the growth of fatigue cracks
6. a railway track may fracture catastrophically at low temperatures under mild overloads
7. a pressure vessel may rupture and leak due to the stable growth of flaws contained in the material

Compromise of structural integrity that originates from elastic and plastic processes can often be prevented by basic design practice based on strength of materials. For failure situations involving plastic deformation, knowledge of material deformation behaviour under service environmental conditions will be required for assessment of integrity. The basic aim in such endeavour is to ensure that sufficient section area is

available to sustain the service stresses and to contain plastic strains within permissible limits. For failure circumstances involving the growth of cracks from pre-existing flaws under the influence of periodic or sustained loading (i.e. failure due to fatigue and by catastrophic or slow fracture), a fracture mechanics based appreciation of the failure process is necessary. This paper attempts to contribute in this regard, by providing an overview of the mechanisms of the growth of cracks and discussing some fundamental issues on the methods that are used to quantify the resistance of materials to such crack extension. The methodologies adopted to assess the integrity of flawed structures from the perspective of fracture mechanics are presented in other papers in this volume.

It may be pointed out that engineering failure through elastic and plastic deformation processes are usually not encountered commonly. This is because of our improved understanding of such processes, and the consequent development of the ability to prevent them. On the other hand, our comprehension and expertise with regards to fatigue and fracture processes are still not mature. This results in the rather large percentage of engineering structural failures through these routes. It is therefore imperative to improve our awareness of how cracks may impair the performance of structures.

Fracture Mechanisms

A fracture mechanism essentially describes the process of fracture. It can be taken to be a bridge between the mechanics aspects of fracture and the material attribute to the science. As mentioned earlier, there are a number of fracture processes, each of which is unique in its own way. The process of unstable crack growth under quasi-static loading conditions is thus somewhat different to the fracture process that is operative during dynamic fracture. Creep crack growth occurs by a mechanism that is not exactly the same as that operating during crack growth under creep-fatigue conditions. There is however quite a large extent of similarity in the mechanisms taking place in these fracture processes, and for the sake of generality it is appropriate that fracture mechanisms be classified into primary types. In the case of a particular fracture process, a combination of such primary fracture mechanisms may be operative, and other specific mechanisms may come into play. Some of such primary fracture mechanisms are: mechanism of fatigue crack growth, ductile fracture mechanism, cleavage fracture and intergranular crack extension. These are discussed below.

Mechanism of Fatigue Crack Growth

A component is said to have failed by *fatigue* when it disintegrates or collapses after having been subjected to a number of cycles of alternating stress. Usually no obvious damage or deterioration in its service capability can be observed throughout the majority of the loading cycles. The magnitude of the cyclic stress applied may be so small that their single application does not result in any detectable damage at all. And the failure surfaces are often apparently brittle, devoid, largely, of gross plastic deformation.

Although fatigue failures may seem to be abrupt, the process of fatigue fracture is progressive, beginning as minute cracks that grow during the service life of components. Sub-microscopic changes take place in the crystalline structure of metals and alloys under the action of repetitive low-level load applications. These minute changes accumulate to lead to the formation of tiny microscopic cracks. The tiny cracks grow under cyclic loading into larger cracks. The larger cracks continue to grow until the stress in the remaining ligament becomes unsustainable, when sudden failure occurs.

The growth history of fatigue cracks can conveniently be sub-divided into stages. Starting from an intrusion/extrusion at the free surface, the crack grows in Stage I at a slant, in a crystallographic fashion. Gradually it deflects into a Stage II crack when a striation forming mechanism dominates. Further on, in Stage III, static fracture modes are superimposed on the growth mechanism, till finally it fails catastrophically by shear at an angle to the direction of growth. Fig.1 gives a schematic representation of the various stages of fatigue crack growth. The surface of Stage II cracks is characteristically covered with parallel markings at intervals of the order of 0.1 μm or more called striations which are supposed to be successive positions of the crack front.

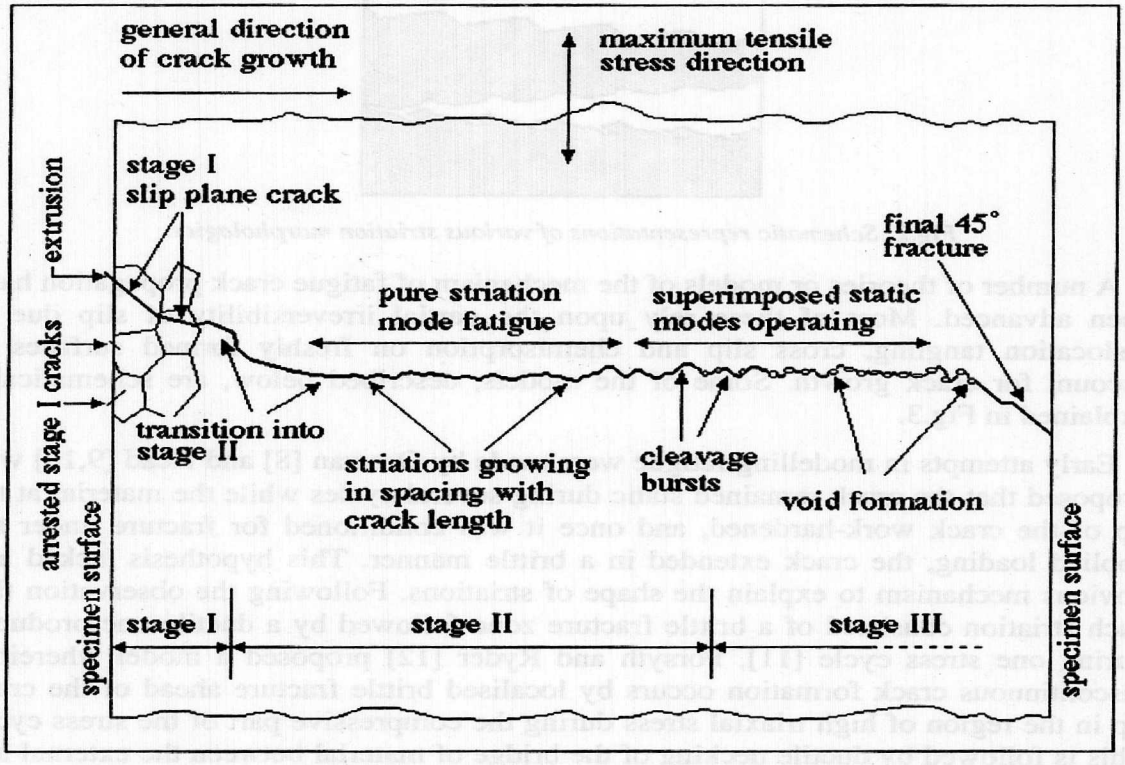

Fig.1: Schematic representation of the various stages of fatigue crack growth.

Evidence for the mechanism of Stage II crack growth has been obtained from studies of striation profiles on fracture surfaces *via* metallographic sections through the crack tip [1–5] and by electron-fractographic examination of failure surface replicas [6,7]. Fig.2 shows schematic representations of the various striation morphologies that have been propounded. The varied nature of striation morphology indicates the variability in the mechanism of fatigue crack propagation.

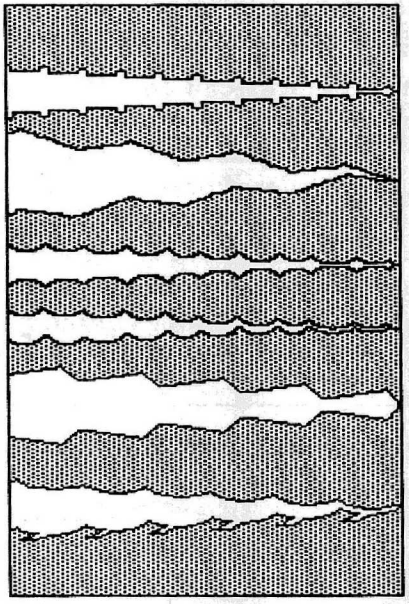

Fig.2: Schematic representations of various striation morphologies.

A number of theories or models of the mechanism of fatigue crack propagation have been advanced. Most of these rely upon the partial irreversibility of slip due to dislocation tangling, cross slip and chemisorption on freshly formed surfaces to account for crack growth. Some of the models, described below, are schematically explained in Fig.3.

Early attempts in modelling fatigue were made by Orowan [8] and Head [9,10] who proposed that the crack remained static during several cycles while the material at the tip of the crack work-hardened, and once it was conditioned for fracture under the applied loading, the crack extended in a brittle manner. This hypothesis lacked any obvious mechanism to explain the shape of striations. Following the observation that each striation consisted of a brittle fracture zone followed by a ductile one produced during one stress cycle [11], Forsyth and Ryder [12] proposed a model wherein a discontinuous crack formation occurs by localised brittle fracture ahead of the crack tip in the region of high triaxial stress during the compressive part of the stress cycle. This is followed by ductile necking of the bridge of material between the external and internal cracks during tensile straining. The model is schematically illustrated in Fig.3.

The ductile necking process might be assumed to produce the characteristic striation morphology.

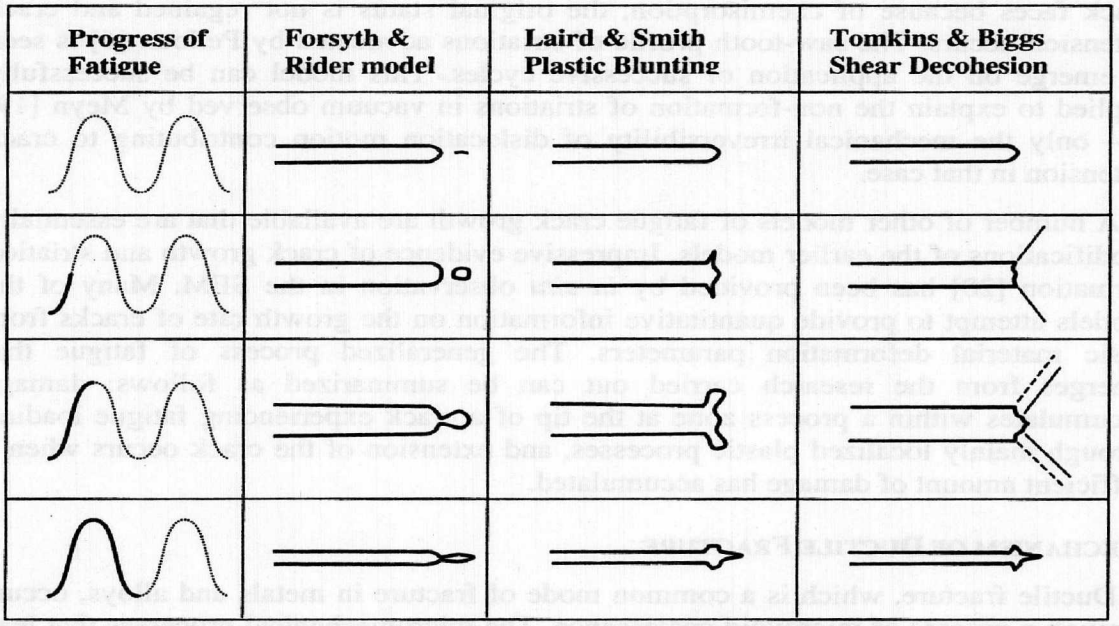

Fig.3: Models of the process of fatigue crack growth

Laird and Smith [13,14], after examination of crack profiles under various stress states of the fatigue cycle in aluminium and nickel, put forward the plastic blunting model. The model essentially involves successive crack tip blunting on the tensile stroke followed by collapse during compression resulting in extension and re-sharpening of the crack. Fig.3 presents a generalised version of the model. From Fig.3 it can be seen that the blunting of the crack tip at maximum tensile load is accompanied by the formation of *ears* on either side of the blunted tip. This characteristic formation is thought to be along plastic deformation bands emanating from the tip and is responsible for the typical shape of striations. Crack extension occurs through outward buckling of the blunted tip. Tomkins and Biggs [15,16] proposed a model, representatively shown in Fig.3, in which shear bands inclined at $\pm 45^{\circ}$ to the crack plane form at the tip of the crack on tensile straining. On further straining, shear decohesion along the inner edges of the shear bands causes the crack tip to blunt and achieve a configuration which, in similarity to the plastic blunting model, would induce crack growth and striation formation.

The alternating shear model, developed by Pelloux [17,18], exhorts alternate slip processes on intersecting slip planes ahead of a crack and relies on the irreversibility of slip during reverse-slip to account for crack extension and the observed striation shape. Initially, as tension is applied to the crack faces, the crack distorts through slip along a predominant slip plane. As back stresses build up on that plane, slip on an intersecting

plane is activated. On reversal of the applied force, reverse slip occurs sequentially. However, due to mechanical irreversibility of slip and prevention of re-welding of the crack faces because of chemisorption, the original status is not regained and crack extension occurs. The saw-tooth profile of striations advocated by Pelloux [6] is seen to emerge on the application of successive cycles. This model can be successfully applied to explain the non-formation of striations in vacuum observed by Meyn [19] — only the mechanical irreversibility of dislocation motion contributing to crack extension in that case.

A number of other models of fatigue crack growth are available that are essentially modifications of the earlier models. Impressive evidence of crack growth and striation formation [20] has been provided by *in situ* observation in the SEM. Many of the models attempt to provide quantitative information on the growth rate of cracks from basic material deformation parameters. The generalized process of fatigue that emerges from the research carried out can be summarized as follows: damage accumulates within a process zone at the tip of a crack experiencing fatigue loading through mainly localized plastic processes, and extension of the crack occurs when a sufficient amount of damage has accumulated.

Mechanism of Ductile Fracture

Ductile fracture, which is a common mode of fracture in metals and alloys, occurs through a process of microvoid coalescence. The micromechanical processes that lead up to the event of ductile fracture are [21]:

a) Initiation or nucleation of voids by the formation of a free surface by interfacial decohesion at, or cracking of, inclusions and second-phase particles.

b) Growth of voids around such inclusions and particles under the action of hydrostatic stress and accumulation of plastic strains.

c) Localisation of strains between growing adjacent voids, resulting in necking and coalescence of adjacent voids.

The mechanism of ductile fracture is schematically illustrated in Fig.4.

In order for voids to be nucleated sufficient stress must be available to break the interfacial bonds between particles and matrix, or to crack the particles. One of the popular models for void initiation was developed by Argon *et al.* [22]. According to this model, void nucleation strain decreases as the hydrostatic stress is increased — a fact that is experimentally justifiable. For nucleation of voids at particles of very small size (<1μm), Goods and Brown [23] have given a dislocation based model that is founded on the fact that dislocation pile-ups at the particle-matrix interface elevate the interfacial stresses responsible for particle-matrix debonding.

After voids have nucleated, their growth and final coalescence depend upon, to a large extent, the density and size distribution of the nucleating particles. It is important to realise that because of the variation in interfacial cohesive strength amongst

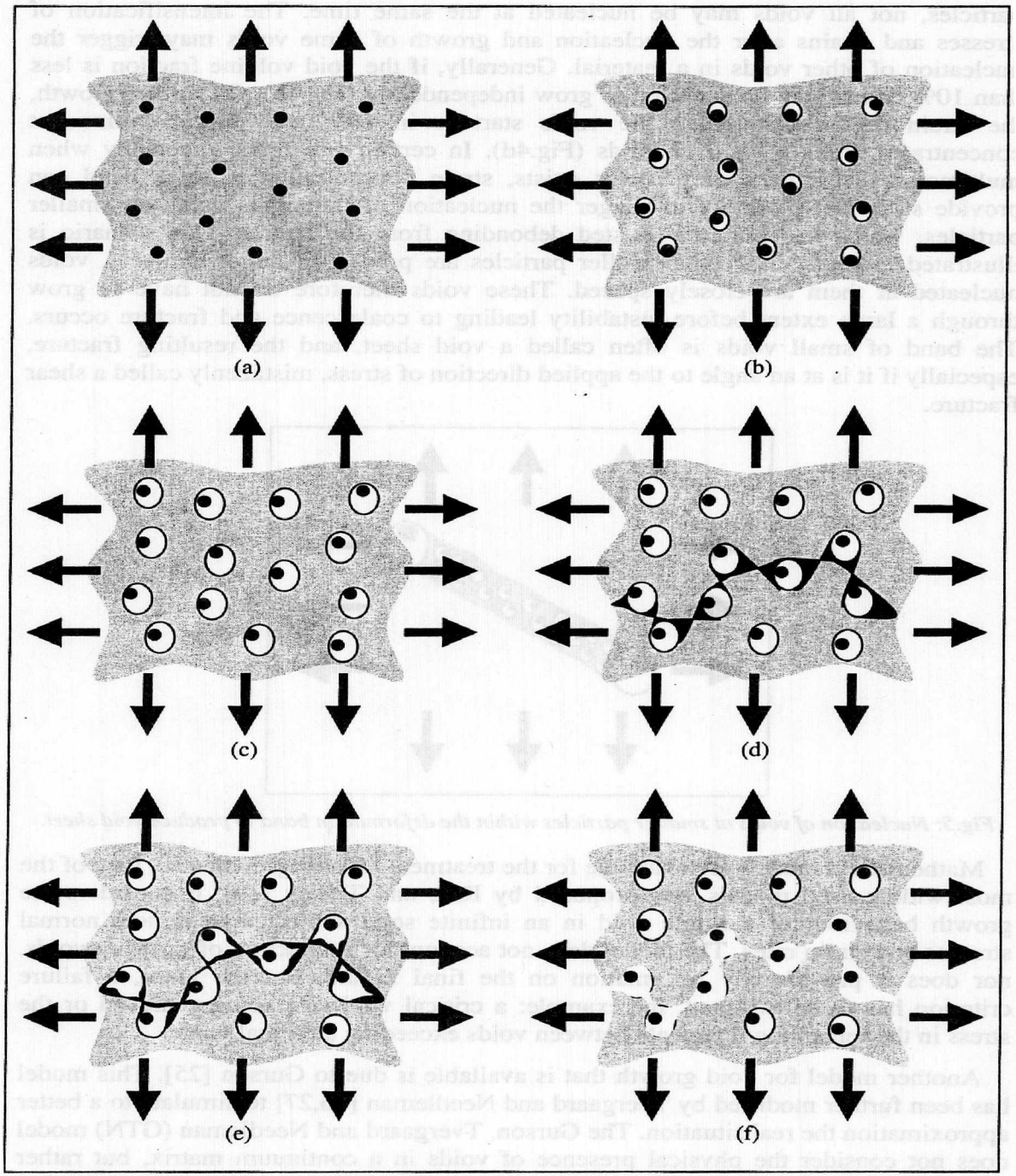

Fig.4: Schematic of the mechanism of ductile fracture through microvoid nucleation, growth and linkage.

particles, not all voids may be nucleated at the same time. The intensification of stresses and strains after the nucleation and growth of some voids may trigger the nucleation of other voids in a material. Generally, if the void volume fraction is less than 10%, voids may be expected to grow independently (Fig.4b). On further growth, the strain fields surrounding the voids start to interact, and plastic strains get concentrated along a band of voids (Fig.4d). In certain situations, especially when multimodal distribution of particles exists, strain concentration along a band can provide sufficient plasticity to trigger the nucleation of numerous voids on smaller particles, which had hitherto resisted debonding from the matrix. This scenario is illustrated in Fig.5. Since the smaller particles are present in larger numbers, voids nucleated at them are closely spaced. These voids therefore do not have to grow through a large extent before instability leading to coalescence and fracture occurs. The band of small voids is often called a void sheet, and the resulting fracture, especially if it is at an angle to the applied direction of stress, mistakenly called a shear fracture.

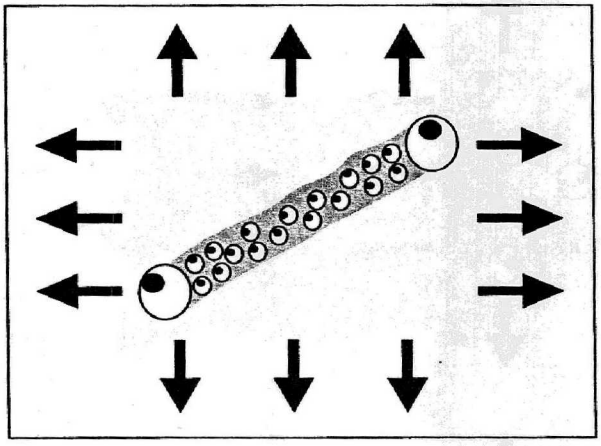

Fig.5: Nucleation of voids at smaller particles within the deformation band to produce void sheet.

Mathematical models are available for the treatment of void growth also. One of the most widely used models was proposed by Rice and Tracey [24]. It considers the growth behaviour of a single void in an infinite solid subjected to remote normal stresses and strain rates. The model does not account for interaction of growing voids, nor does it provide any information on the final failure. For the latter, a failure criterion has to be assumed, for example: a critical void size being achieved or the stress in the remaining ligaments between voids exceeding a critical value.

Another model for void growth that is available is due to Gurson [25]. This model has been further modified by Tvergaard and Needleman [26,27] to simulate to a better approximation the real situation. The Gurson, Tvergaard and Needleman (GTN) model does not consider the physical presence of voids in a continuum matrix, but rather assumes a porous medium to act as a continuum. The GTN model provides a number of parameters that may be calibrated in order to portray not only void growth, but also void coalescence and fracture.

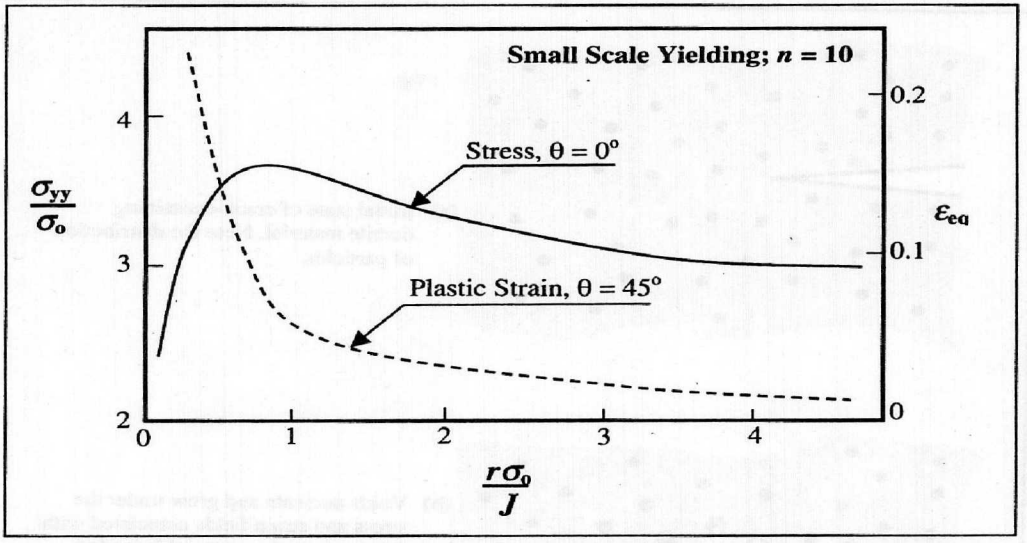

Fig.6: Nature of crack tip stress and strain fields in a strain hardening ductile material.

When a ductile material containing a crack is loaded, stress and strain fields develop in the crack tip region. Under the influence of these fields, the crack tip blunts and this further affects the nature of the stress and strain fields. When sufficient plasticity has engulfed the crack tip, the nature of the stress and strain fields just ahead of the crack tip in strain-hardening materials is typically given by Fig.6. Note that the stress field is capped at ~$3.5\sigma_o$ (σ_o is the flow stress), while the equivalent strain field (at 45° to the crack plane) exhibits a singularity. Under the stress and strain fields shown in Fig.6, and due to the stress triaxiality (which ensures high hydrostatic stress) provided by the crack configuration, microvoids nucleate and grow ahead of the crack. These voids ultimately merge with the crack tip, resulting in crack extension through ductile fracture. The process is schematically illustrated in Fig.7. Ductile fracture from pre-existing cracks in real materials has been modelled using both the Rice and Tracey approach [28] and the GTN approach [29]. Such modelling have shown excellent correlation with experimental *J*-resistance curve data.

CLEAVAGE FRACTURE

The rapid propagation of cracks along preferential planes is called cleavage fracture. Such fractures usually occur through the breaking of interatomic bonds between crystallographic planes. The fracture appears brittle without the manifestation of plastic deformation. The favoured crystal structures for cleavage are those that offer planes with lowest packing density, so that a minimum number of atomic bonds have to be broken, and those that provide fewer active slip systems. Cleavage fracture therefore occurs readily in BCC materials along {100} planes, but is rare in FCC structures in which plastic deformation is encouraged through a large number of slip systems. It is consequently a potent mechanism of fracture in ferritic steels.

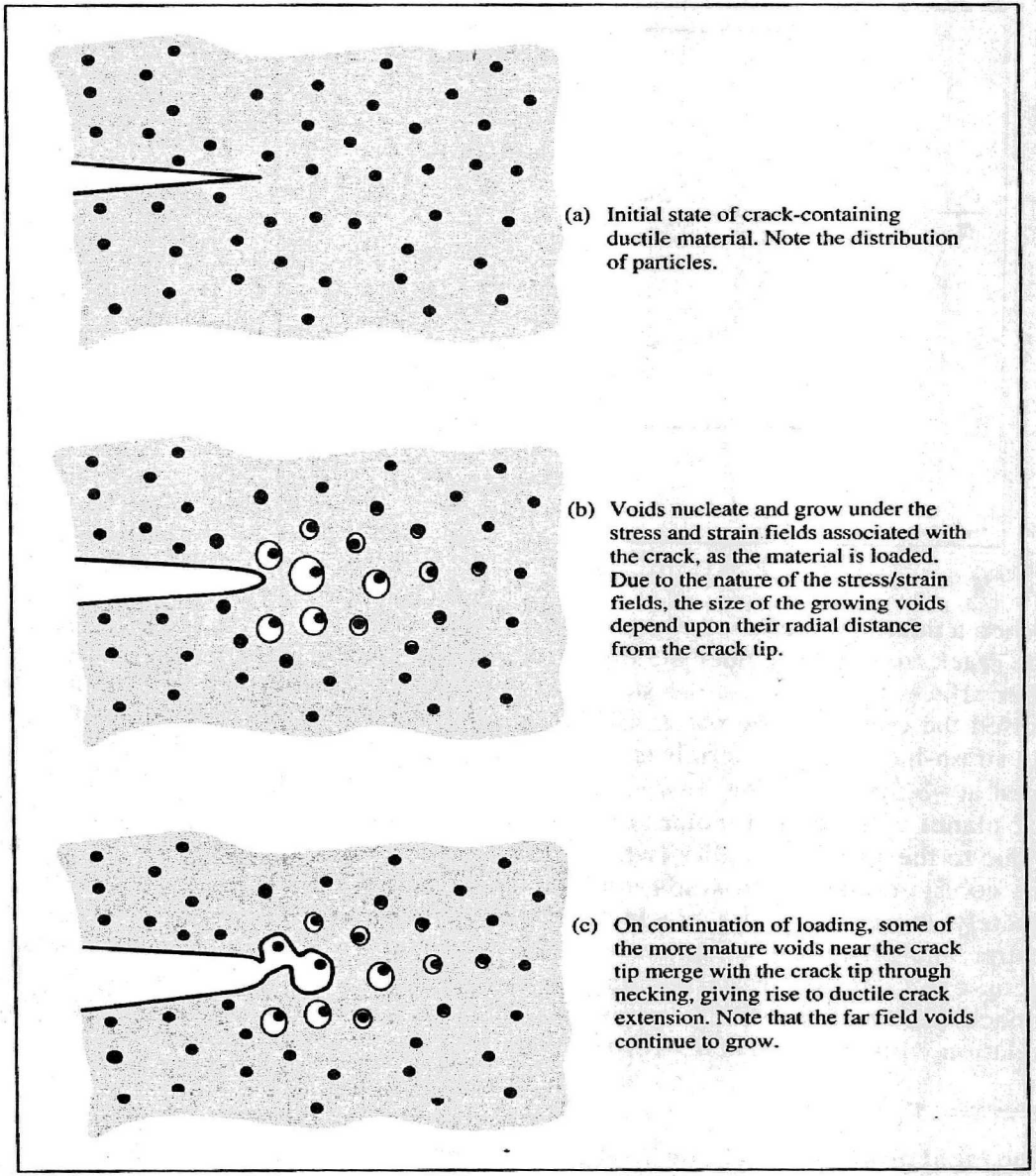

Fig.7: Mechanism of ductile crack extension through void initiation, growth and coalescence with crack tip.

When cleavage fracture occurs in polycrystalline materials, misorientations of cleavage planes in neighbouring grains results in the tilting of the transgranular crack as it passes through the material. In a 3-D situation, twisting of the crack plane may also be required in order to ensure growth along preferred planes. To facilitate accommodation of such twists, a cleavage crack grows along several parallel planes that are joined by tearing between the planes. However as such cross-plane tearing is

not energetically favourable, multiple cracks along the several planes tend to converge into a single plane. This mechanism results in the formation of typical cleavage fracture feature called *riverlines*. The situation is schematically illustrated in Fig.8. It is clear from the figure that the direction of cleavage crack propagation may be inferred from a study of the pattern of riverlines.

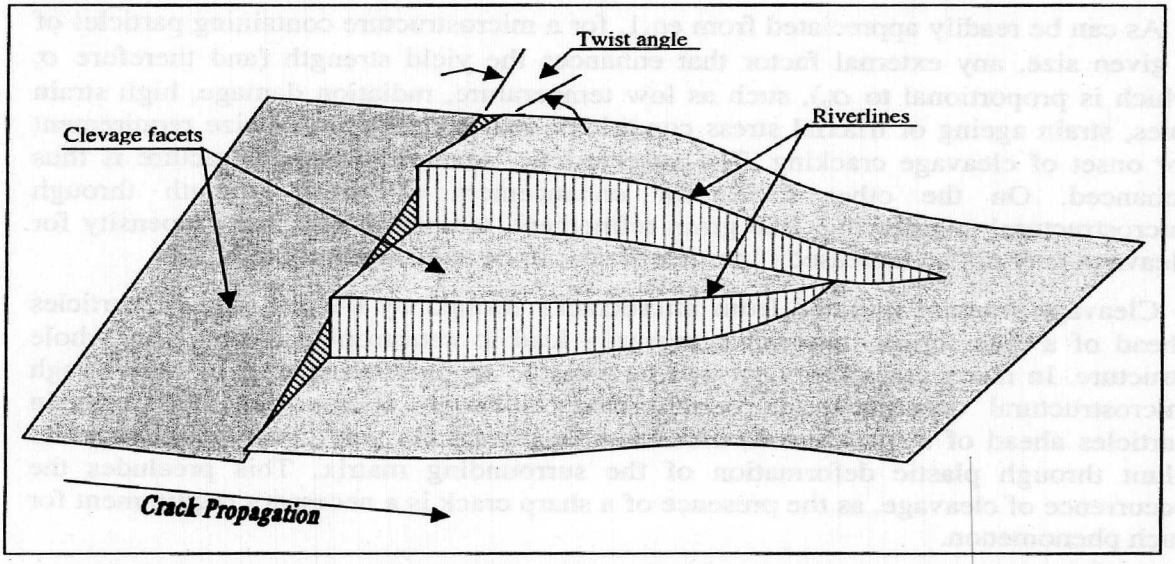

Fig.8: Schematic of riverline patterns that are formed when cleavage cracks cross over twist boundaries between grains.

As mentioned above, cleavage fracture occurs through breakage of inter-planar atomic bonds. The stress required to break such bonds is of the order of E/π, whereas the maximum stress available ahead of a crack in a strain hardening material is about $3.5\sigma_o$ as shown in Fig.6, which is ~50 times less than the required value. Thus the stress concentration provided by a macroscopic crack is insufficient to cause cleavage fracture autogenously. The stress field of a macroscopic crack is often sufficient however to nucleate a sharp microcrack in favourably located brittle microscopic particles and inclusions. If such microcracks are of adequate size, they may extend into the surrounding matrix by cleavage under the action of the remote stress generated by the macrocrack due to the satisfaction of Griffith's energy balance criterion. It can be said therefore that the onset of cleavage cracking is brought about by the cracking of brittle particles in the microstructure. If it is assumed that a penny shaped crack is formed by the cracking of spherical second phase particles of diameter C_o, then, invoking the Griffith energy balance criterion for crack extension, it can be written that

$$C_o = \frac{\pi E \gamma_p}{(1-\nu^2)\sigma_r^2} \qquad \ldots (1)$$

for the case of propagation of a cleavage crack. In the above equation σ_r is the stress created by the macrocrack and γ_p is the plastic work required to create a unit area of

cleavage fracture surface. It is assumed that the cleavage surface energy is negligible compared to γ_p. For typical ferritic steel with an estimated γ_p of 14 J/m^2 [21], particles should be of at least ~7 μm diameter, as per the above equation, in order to trigger the onset of cleavage fracture. Brittle particles of this size are indeed a possibility in commercial grades of steels.

As can be readily appreciated from eq.1, for a microstructure containing particles of a given size, any external factor that enhances the yield strength (and therefore σ_r which is proportional to σ_o), such as low temperature, radiation damage, high strain rates, strain ageing or triaxial stress conditions, reduces the particle size requirement for onset of cleavage cracking. The susceptibility towards cleavage fracture is thus enhanced. On the other hand, for enhancement of yield strength through microstructural engineering, like grain refinement, tempering etc., the propensity for cleavage may not be increased if particle sizes can be concomitantly reduced.

Cleavage fracture initiated from microcracks formed by the splitting of particles ahead of a macrocrack may not necessarily lead to catastrophic failure of a whole structure. In many cases cleavage will be arrested at grain boundaries or other tough microstructural constituent. In certain cases although microcracks will form in particles ahead of a macrocrack, unfavourable conditions may cause such cracks to blunt through plastic deformation of the surrounding matrix. This precludes the occurrence of cleavage, as the presence of a sharp crack is a necessary requirement for such phenomenon.

Since the perception of cleavage fracture in metallic materials is essentially based upon the concept of formation of microcracks in brittle second phase particles, the statistical probability of presence of a particle of the right size at the right location is important. A large volume of research has been carried out in understanding and quantifying this statistics, particularly with reference to ferritic steel systems. The model proposed by Ritchie, Knott and Rice [30] is a milestone in this regard that promulgated the application of the weakest link phenomenon in understanding the mechanism of cleavage fracture.

INTERGRANULAR FRACTURE MECHANISMS

Ductile void growth and cleavage are the preferred mode of fracture in metals and alloys. However, intergranular fracture through the propagation of cracks along grain boundaries may occur under the influence of the external environment. Such fractures have the typical "rock candy" appearance. Depending upon the nature of the environment and its interaction with a metallic system under stress, a variety of mechanisms may be responsible for intergranular fracture. Some of them are:

1. Precipitation of brittle phases on grain boundaries during solidification or heat treatment.
2. Segregation of embrittling species to grain boundaries (often dynamically) under the influence of high temperatures and stress.

3. Hydrogen embrittlement and environmentally assisted cracking.
4. Intergranular corrosion.
5. Cavitation and cracking of grain boundaries at elevated temperatures.

Improper heat treatment of metallic alloys may result in the precipitation of brittle phases and particles along grain boundaries. These fracture or decohese preferentially under the stress field of existing cracks or flaws which then find it energetically favourable to grow along the grain boundaries. An example of this is the intergranular fracture of steels which have been temper embrittled because of tempering at ~500°C. Low alloy steels in service at elevated temperatures are known to exhibit stress-assisted dynamic segregation of embrittling elements like P, S *etc.* to grain boundaries under the influence of stress fields of cracks [31]. Coverage of grain boundary surfaces by these elements reduces their cohesive strength so that intergranular fracture ensues.

Hydrogen embrittlement and environmentally assisted cracking are both manifestations of the effect of hydrogen on the integrity of materials. Both these mechanisms are still not understood well. The essential sequence of events that lead to the process of embrittlement and crack extension may be listed as follows:

a) Transport of deleterious environment containing hydrogen to the crack tip.
b) Reaction of the environment with the material at the crack tip resulting in the evolution of atomic hydrogen that is absorbed into the material.
c) Diffusion of elemental hydrogen, often under the influence of crack tip stress fields, to favourable sites ahead of the crack tip.
d) Hydrogen-metal interaction at such sites leading to embrittlement and crack growth.

It may be noted that it is not necessary that the processes listed above will always lead to intergranular fracture. The grain boundary is simply a favourable site to which hydrogen may diffuse causing the reduction of cohesive strength.

For hydrogen embrittlement to occur, hydrogen may be picked up from a variety of sources at ambient or elevated temperatures, like H_2 gas, H_2S, moisture, steam, sour crude *etc.* Environmentally assisted cracking usually involves not only hydrogen pick-up from the crack tip, but also other electrochemical reactions at the crack tip, often in an aqueous media. In intergranular corrosion, the embrittling aspect in the process of fracture is absent. Intensive corrosion takes place preferentially at grain boundaries, usually due to electrochemical reasons, leading to the reduction of resistance to intergranular growth of a crack.

At high temperatures, the cohesive strength of grain boundaries is compromised so that they are often weaker than the matrix of the grains. This is why creep deformations are often accommodated by grain boundary cavitation and sliding along grain boundaries. Many fractures that take place at high temperatures are intergranular because intensive creep processes are activated.

The fracture mechanisms discussed above are the common mechanisms observed primarily in metallic materials. In non-metals and advanced materials, several other mechanisms that are distinctly different to the above come into play. Discussions on them are outside the scope of this paper; however, for fracture mechanics based assessment of performance of such materials, appreciation and awareness of such mechanisms are also necessary. The review by Anderson [32] may be referred to for an overview on these issues.

Fracture Resistance of Materials

Since fracture through formation and growth of cracks is a potent method of degradation of structural integrity, it is necessary to determine the resistance which materials offer to this process. Fracture resistance can be determined by a variety of means. Table 1 lists the various methods that are available as ASTM standards for the quantification of fracture and fatigue resistance. Other organisations like ISO, DIN, BSI, JIS *etc.* have also published similar standard test methods. The ASTM standard test methods can be divided into two categories, as shown in Table 1. The first category of tests are conducted on smooth specimens or on specimens that contain notches or crack starters to act as stress concentrators to localise the formation of cracks. These tests therefore provide information on not just fracture resistance, but also on the resistance offered by deformation processes that (macroscopically) pre-condition the material for fracture. Many of the tests (e.g. E23, E208, E436) are often used from a comparative standpoint (a *go, no-go* verification), in which a minimum value or other characteristic, like fracture appearance, must be surpassed in order for a material to be qualified for engineering use. The second category of tests uses specimens in which cracks are introduced *a priori* to the test. They therefore reveal the behaviour of materials that already contain cracks — a scenario that is increasingly being used for the assessment of integrity of structures, and elicit the resistance provided mainly by the process of fracture (and associated *localized* deformation processes). Most of the tests in this category are of relatively recent origin, and are based on the principles of fracture mechanics. Some of the more important fracture mechanics based test methods are highlighted in Table 1. The discussion in this paper is restricted to this group. It may be pointed out that the development of standards on quantification of fracture resistance is concomitant with developments in the philosophy of preventing fractures.

Fracture Mechanics based Quantification of Fracture Resistance

For measurement of fracture resistance (better known as fracture toughness) under monotonically increasing loads using fracture mechanics principles, the methods described in the ASTM standards E399, E813, E1290 and E1737 may be followed. ASTM standard E647 is used for the quantification of resistance to fracture through fatigue. A full discussion on the testing methods is not attempted in this paper; reference should be made to the standards to obtain information in this regard [33-37]. Here discussions are limited to some of the salient features of the test methods and the fracture mechanics basis for the procedures.

Table 1: ASTM standards available for the establishment of fracture and fatigue properties

Category 1	E466	Conducting constant amplitude axial fatigue tests of metallic materials
	E606	Constant amplitude low-cycle fatigue testing
	E338	Sharp-notch tension testing of high strength sheet materials
	E602	Sharp-notch tension testing with cylindrical specimens
	E208	Conducting drop weight test to determine nil-ductility transition temperatures of ferritic steels
	E23	Notched bar impact testing of metallic materials
	E436	Drop weight test of ferritic steels
	E604	Dynamic tear testing of metallic materials
	E1304	Plane strain chevron-notch fracture toughness of metallic materials
Category 2	E812	Crack strength of slow bend pre-cracked Charpy specimens of high strength metallic materials
	E992	Determination of fracture toughness of steels using equivalent energy methodology
	E740	Fracture testing with surface crack tension specimens
	E399	Plane strain fracture toughness of metallic materials
	E1290	Fracture toughness measurement crack tip opening displacement (CTOD)
	E813	J_{Ic}, a measure of fracture toughness
	E1152	Determining J-R curves
	E561	R-curve determination
	E1737	J-integral characterization of fracture toughness
	E1221	Determining the plane strain crack arrest fracture toughness, K_{Ia}, of ferritic steels
	E1457	Measurement of creep crack growth rates in metals
	E647	Measurement of fatigue crack growth rates

The various types of fracture mechanics specimens that are commonly used and their mode of loading are shown in Fig.9. The standards to which the specimens are applicable are noted in the figure. From the standpoint of fracture mechanics however, any specimen geometry can be used for any of the fracture mechanics based tests. All specimen geometry contain a notch from which a pre-crack must be grown under fatigue loading prior to testing. The notch is therefore provided with a sharp tip to ensure easy initiation of fatigue pre-cracks. Sometimes a chevron notch is used for easy initiation of cracks and restricting the pre-cracks to the plane of the notch. Often in fracture toughness testing with ductile materials, side-grooves are machined on the specimen flanks after pre-cracking to prevent crack meandering.

An important and universal requirement in most fracture mechanics based tests is the measurement of crack length during the progress of tests. Cracks may be monitored by a variety of methods (see [38] for an overview). Some of the popular

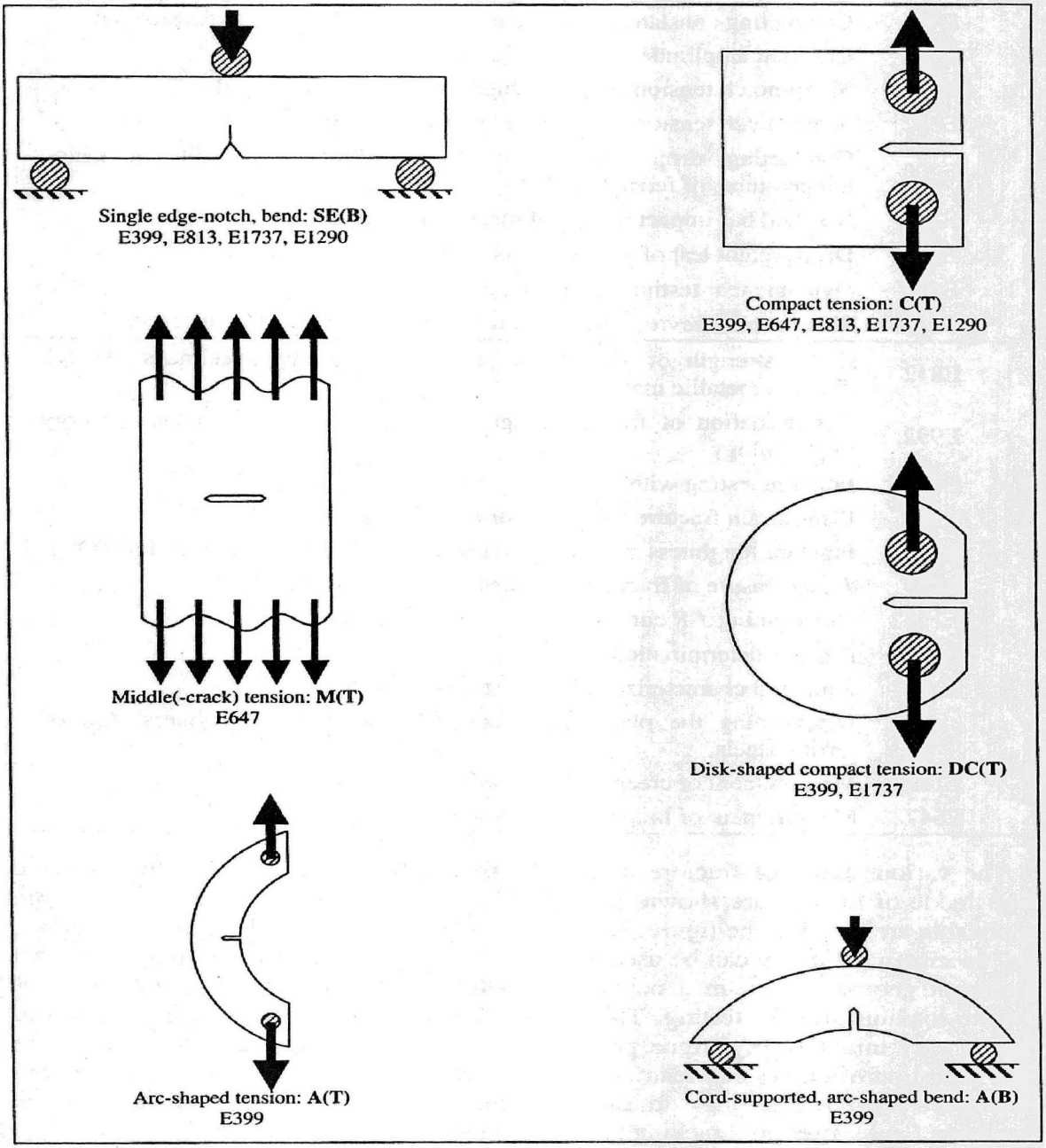

Fig.9: Specimen geometries available for carrying out fracture machanics based tests for the measurement of fracture resistance.

methods are: visual measurement using optical devices like telescopes, the potential drop method and the compliance method. The last two methods are amenable to

on-line automatic implementation leading to computer-interfaced feedback controlled automated testing. In the potential drop method, a d.c. or a.c. voltage is applied across the specimen, remote from the crack tip. The potential difference in the vicinity of the crack is measured, usually across the mouth of the notch, and the crack length in the specimen is calculated from this. Correlations of voltage measured and crack length are available in the literature [39] for carrying out such calculations. In the compliance technique, periodic elastic unloading through a small load range is imposed on the specimen during testing. From the load and displacement — usually crack mouth opening displacement (CMOD) measured by attaching a CMOD gauge (or COD gauge as it is more popularly known), data, the elastic compliance (given by displacement/load; inverse of stiffness) is calculated. For fatigue crack growth tests (E647), the load and displacement data obtained during fatigue cycling can be used to compute the compliance. Specimen geometry specific correlations (called compliance crack length relations) are available in the literature [40,41] for calculating the crack length from the elastic compliance.

FRACTURE TOUGHNESS AND THE CONCEPT OF *R*-CURVE

In fracture mechanics, the concept of a resistance curve or *R*-curve is used to represent a material's resistance to the propagation of cracks. The *R*-curve is assumed to be independent of crack length and, under ideal situations (clarified later), the *R*-curve for a crack-containing structure can be represented as shown in Fig.10a. When such a structure is subjected to increasing stresses, the driving force ($\mathcal{G}$) tending to extend the crack increases as also shown in Fig.10a. The driving force is proportional to the length of the crack and the magnitude of the applied stress. The crack in the structure will start to propagate when the driving force exceeds the critical resistance. With reference to Fig.10a, the driving force curve for an applied stress of σ_1 does not cause crack propagation for the given crack length because it is lower than the critical R of the material. The driving force for an applied stress of σ_2 just overcomes the critical resistance and results in unstable crack extension.

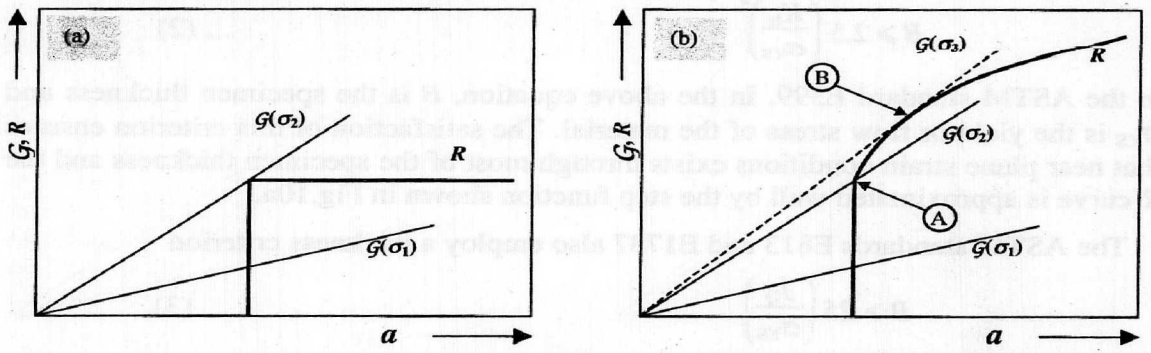

Fig.10: Fracture mechanics concept of resistance curves and crack driving force curves

R-curves as in Fig.10a, which are of the form of a step function, are exhibited by materials under ideal conditions of plane strain in which a very high degree of stress

triaxiality accompanied by very little plasticity exists. Due to the nature of the R-curve (a constant resistance to crack extension), it can be appreciated that a singular critical fracture resistance parameter (or fracture toughness) can be ascribed to the material. The fracture toughness parameters K_{Ic} and δ_{Ic} obtained by the methods described in the ASTM standards E399 and E1290 respectively, are most appropriate for this. The crack driving parameters K (stress intensity factor, SIF) and δ (crack-tip opening displacement, CTOD) are used for representing the crack driving force curves in the two cases.

More often than not, a material's R-curve is rarely in the form portrayed in Fig.10a. A rising R-curve, as shown in Fig.10b, is often observed in which crack extension is initiated on exceeding a critical resistance (point A in Fig.10b), but continued extension of the crack requires increasing amount of resistance to be overcome. A crack driving force obtained under an applied stress of σ_2 therefore is able to initiate crack extension, being equal to the resistance at point A, but is not able to sustain crack growth, as the crack driving force curve beyond point A is lower than the resistance curve of the material. Under an applied stress of σ_3 however unstable crack growth can ensue since the driving force curve is tangential to the resistance curve at point B. For situations of this type, a singular fracture toughness parameter is not very helpful, and fracture resistance through a range of crack extension has to be characterised. The J-integral is used for this in the ASTM standards E813 and E1737.

A rising R-curve is exhibited under conditions of plane stress. In reality, the stress triaxiality ahead of a crack tip will vary from the surface of a specimen to the centre. The surface of the specimen will be in plane stress due to substantial plastic yielding in such regions, while, depending on the deformation behaviour of the material and the specimen thickness, plane strain may be exhibited in the central region. The contribution of the plane stress regions at the surface causes the R-curve to have a rising tendency. The suitability of K_{Ic} to characterise a material's fracture resistance is therefore judged by using a thickness criterion

$$B \geqslant 2.5\left(\frac{K_{Ic}}{\sigma_{YS}}\right)^2 \qquad \ldots (2)$$

in the ASTM standard E399. In the above equation, B is the specimen thickness and σ_{YS} is the yield or flow stress of the material. The satisfaction of this criterion ensures that near plane strain conditions exists through most of the specimen thickness and the R-curve is approximated well by the step function shown in Fig.10a.

The ASTM standards E813 and E1737 also employ a thickness criterion

$$B \geqslant 25\left(\frac{J_Q}{\sigma_{YS}}\right) \qquad \ldots (3)$$

to qualify a critical value of J (J_Q) as the ductile fracture toughness J_{Ic}. J_Q is identified in the rising R-curve at a point corresponding to 0.2 mm of ductile crack extension. The thickness criterion of eq.3 ensure that an optimum amount of stress triaxiality exists at the crack tip so that a size independent lower-bound ductile fracture toughness

is obtained, despite the greater plasticity and the consequent rising R-curve. The analysis procedures contained in the J-integral based standards also produce the complete R-curve as a plot of J against crack extension, Δa (sometimes called the J-R or J_R curve).

The above discussion on R-curves can be summarised and further substantiated as follows:

1. The crack extension resistance curve of a material, although a material property, may be modified by the stress triaxiality at the crack tip. The stress triaxiality, in turn, is governed by the amount of plastic deformation in the crack tip region.
2. For a situation of high stress triaxiality, the R-curve may be approximated by a step-function, and the critical resistance to fracture or fracture toughness characterised by a singular parameter like K_{Ic} or δ_{Ic}.
3. When the stress triaxiality is relaxed through plastic deformation in the crack tip region, a rising R-curve is exhibited. J is the preferred parameter to characterise such a rising R-curve. A ductile fracture toughness, J_{Ic}, can still be used to describe the material's resistance to crack propagation provided the crack tip plasticity is well contained and a minimum amount stress triaxiality exists at the crack tip.

It is clear that the high stress triaxiality fracture toughness parameters K_{Ic} and δ_{Ic} permit very little or no plasticity to occur at the crack tip. The material therefore behaves macroscopically in an elastic manner, and the parameters are known as linear-elastic fracture mechanics (LEFM) parameters. J, on the other hand, can be used for conditions of lower triaxiality when the plasticity at the crack tip can be substantial, and therefore it is known as an elastic-plastic fracture mechanics (EPFM) parameter.

Since the plasticity attending the crack tip under LEFM conditions is insignificant, it can be assumed that ductile fracture processes through microvoid coalescence will not be operative when K_{Ic} is applicable. Brittle fracture through cleavage cracking will be the preferred mode of fracture. Conversely, under EPFM conditions, when J is used to characterise fracture resistance, failure will normally occur through the ductile microvoid initiation and growth mechanisms as extensive plastic deformation is required for such processes. There will be cases however, when substantial plastic deformation must be imposed prior to the onset of brittle cleavage fracture, or when ductile voidous fracture is interspersed with cleavage bursts. Generally, in addition to imposed fracture mechanics conditions, the local microstructure controls the micromechanism of fracture.

FRACTURE TOUGHNESS TEST METHODS

LEFM test methods (E399) essentially consist of loading a fracture mechanics specimen to failure under displacement control. During the test, the load on the specimen and the displacement at the load points or, preferably, at the crack mouth are monitored. From a plot of load against displacement, the critical load corresponding to the onset of crack extension is identified. Due to the nature of the R-curve (i.e. a step-

function), a deleterious drop in load (called a "pop-in" from the audible acoustic accompanying the crack-burst) occurs at this point, as crack extension is unstable. From the identified critical load (P), K_{Ic} is calculated using SIF expressions, provided the relation in eq.2 and other criteria are satisfied. SIF expressions are available in the standards, and are of the form

$$K = \frac{P}{B} F(W) f\left(\frac{a}{W}\right) \quad \ldots (4)$$

where f and F are functions, B and W are the specimen thickness and width respectively, and a is the crack length with which the fracture toughness test is carried out. In case the critical load cannot be identified unambiguously, as when the R-curve exhibiting a slightly rising tendency, the E399 standard provides alternative procedures to obtain an operationally acceptable fracture toughness value.

In EPFM testing (E813, E1737), fracture mechanics specimens are loaded under displacement control up to appreciable amounts of tearing crack extension. In addition to the load and load-point displacement, the growth of the crack must also be monitored in these tests. If a visual method of crack extension measurement (Δa) is to be used, multiple specimens are necessary for constructing the J-R curve, a different amount of Δa being allowed in each specimen. Alternatively, a single specimen technique is advocated by standards wherein potential drop or compliance is used for measuring Δa continuously during the test. At any instant of ductile or tearing crack extension, the J-integral is equivalent to the rate of change in strain energy (U) with increase in crack length (a) per unit specimen thickness (B), approximating the elastic-plastic flow behaviour of the material as a non-linear elastic phenomenon. Mathematically this can be represented by

$$J = -\frac{1}{B}\left(\frac{\partial U}{\partial a}\right) \quad \ldots (5)$$

In a test, J is calculated from the area (A) under the load (P) versus plastic load-point displacement (Δ_p) curve using an equation of the form

$$J = \frac{2A}{B\,(W\text{-}a)}\,\mathbf{F} \quad \ldots (6)$$

where **F** is a function dependent on the geometry of the specimen. Contributions of elastic loading to J and corrections for specimen rotation and growth of the crack during testing have to be applied to the computed J; details can be found in the ASTM standards. The J-R curve is given by a plot of J against Δa, and the total curve represents the resistance of the material to ductile crack extension. This curve is often necessary for design and integrity assessment purposes. From the curve, through an elaborate qualification and iterative scheme, a J_{Ic} may also be defined.

FATIGUE CRACK GROWTH TESTS

Fatigue crack growth rate (FCGR) tests as per ASTM standard E647 report the crack growth rate per cycle, da/dN, as a function of the stress intensity factor range ΔK. A fracture mechanics specimen is subjected to cyclic loading employing, usually, a sinusoidal waveform. The amplitude of the cyclic loading (ΔP) is used in conjunction with the relevant SIF expression of the form given in eq.4 to calculate ΔK. The mean level of the load cycle is described by the R-ratio, which is the ratio of the minimum load (P_{min}) to the maximum load (P_{max}), or equivalently the ratio of the corresponding SIFs, K_{min}/K_{max}. Two variants of the FCGR test are allowed by the standards: a constant load amplitude test and the decreasing ΔK test. In the former, ΔP is kept constant throughout the duration of the test, resulting in the natural increase of ΔK as the crack length a increases. In the latter type of test, ΔP is decreased progressively with crack growth so that ΔK is made to decrease as per the relation

$$\Delta K = \Delta K_o \, e^{C(a-a_o)} \qquad \ldots (7)$$

where ΔK_o and a_o are the initial ΔK and a with which the test is started, and C is a constant equal to –0.08/mm. With respect to a plot of da/dN versus ΔK, the first type of test obtains the data from a lower to a higher value of ΔK, while the second type of test obtains the data in the reverse order. The second type of test is especially useful for obtaining crack growth resistance data at low values of ΔK (say, in the threshold regime; see Fig.11) at which it would be difficult to initiate a crack employing the first method of constant ΔP. An alternative method of conducting decreasing ΔK tests employing a different philosophy and relation of reducing ΔK to that given in eq.7 is also available [42].

One of the most important aspect of FCGR testing is monitoring crack length as the crack grows under fatigue loading. With the advances available in computer based automation, the potential drop method or the compliance technique is recommended. The essential data to be obtained from a FCGR test consists of a and number of cycles (N), in addition to ΔP. For calculating ΔK, a and ΔP data are necessary. The (a, N) data are differentiated numerically to obtain da/dN. For this the E647 standard advocates the use of an incremental polynomial method.

A schematic output from a FCGR test is shown in Fig.11. The (da/dN, ΔK) data are plotted in log-log axes to result in a typical sigmoidal plot for a full range of growth rates, from 10^{-8} to 10^{-3} mm/cycle. Such plots are often called Paris plot after Paris and Erdogan [43], who popularised the representation of fatigue crack growth resistance in this manner. Paris plots can characteristically be sub-divided into three regimes of crack growth as shown in Fig.11. The threshold regime represents the behaviour of cracks under low levels of crack driving forces, and is bounded on the lower side by the threshold ΔK, ΔK_{th}, that corresponds to the lowest crack driving force which can result in crack extension under fatigue. ΔK_{th} is often an important parameter from the point of view of design and integrity assessment, and the derivation of ΔK_{th} is often the objective of FCGR tests. The central regime of crack growth is called the Paris regime

and the growth rates in this region can be represented by the relation which was proposed by Paris and Erdogan [43]

$$\frac{da}{dN} = C\,\Delta K^m \qquad \ldots (8)$$

where C and m are material constants.

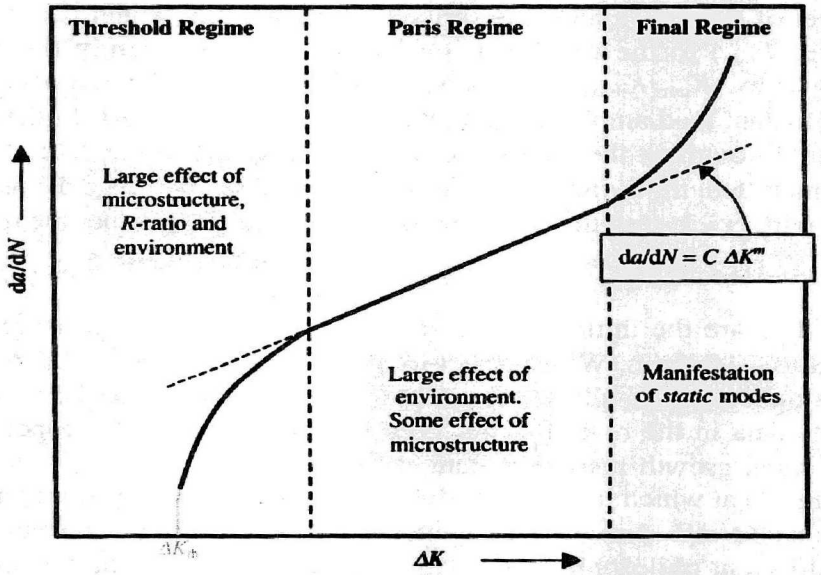

Fig.11: Schematic of fatigue crack growth resistance curve, also known as Paris plots

CONCLUDING REMARKS

For the purpose of integrity assessment of structural components that are prone to disintegration through the formation and growth of cracks or in which crack-like flaws have been identified, fracture mechanics principles have to be employed. For the successful implementation of fracture mechanics based methodology to such situations, an understanding of the process of fracture and the resistance offered by materials to such processes is required. The present paper provides a basic background to developing such understanding.

The importance of establishing a link between the microstructure of a material and the processes that threatens the integrity of a component made of the material cannot be overemphasized. It has not been possible to discuss much on this issue within the scope of this paper. Similarly, the significance of fracture mechanics based destructive test techniques in the process of integrity assessment has not been touched upon in this paper. The reader is referred to the guidelines that are available from professional organisation in this regard [44-45]. Other papers in this volume also highlight the requirement of fracture mechanics test data.

REFERENCES

1. C.A. Stubbington, *Metallurgia*, **68** (1963), 109
2. P.J.E. Forsyth, *Acta Met.*, **11** (1963), 703
3. C. Laird, "Studies of High-strain Fatigue", Ph.D. Thesis, University of Cambridge, 1962
4. C. Laird, ASTM STP **415**, Am. Soc. Testing Mat., Pa., 1967, p.131
5. A.J. McEvily Jr. and T.L. Johnston, *Int. J. Fracture Mech.*, **3** (1967), 45
6. J.C. McMillan and R.M.N. Pelloux, ASTM STP **415**, Am. Soc. Testing Mat., Pa., 1967, p.505
7. R.W. Hertzberg, ASTM STP **415**, Am. Soc. Testing Mat., Pa., 1967, p.45
8. E. Orowan, *Proc. Royal Soc. A*, **171** (1939), 79
9. A.K. Head, *Phil. Mag.*, **44** (1953), 925
10. A.K. Head, *J. Appl. Mech.*, **78** (1956), 407
11. P.J.E. Forsyth, C.A. Stubbington and D. Clark, *J. Inst. Metals*, **90** (1961-62), 238
12. P.J.E. Forsyth and D.A. Ryder, *Metallurgia*, **63** (1961), 117
13. C. Laird and G.C. Smith, *Phil. Mag.*, **7** (1962), 847
14. C. Laird and G.C. Smith, *Phil. Mag.* **8** (1963), 1945
15. B. Tomkins and W.D. Biggs, *J. Mat. Sci.*, **4** (1969), 544
16. B. Tomkins, *Phil. Mag.*, **18** (1968), 1041
17. R.M.N. Pelloux, *Eng. Fracture Mech.*, **1** (1970), 697
18. R.M.N. Pelloux, *Trans. ASM*, **62** (1969), 281
19. D.A. Meyn, *Trans. ASM*, **61** (1968), 52
20. H. Vehoff and P. Neumann, *Acta Met.*, **27** (1979), 915
21. J.F. Knott, "Micromechanism of fracture and fracture toughness of engineering alloys", Proc. ICF4, Waterloo, Canada, 1977, pp.61-91
22. A.S. Argon, J. Im and R. Safoglu, "Cavity formation from inclusions in ductile fracture", *Met. Trans.*, **6A** (1975), pp.825-837
23. S.H. Goods and L.M. Brown, "The nucleation of cavities by plastic deformation", *Acta Met.*, **27** (1979), pp.1-15
24. J.R. Rice and D.M. Tracey, "On the ductile enlargement of voids in triaxial stress fields", *J. Mech. Phys. Solids*, **17** (1969), pp.201-217
25. A.L. Gurson, "Continuum theory of ductile rupture by void nucleation and growth: part I — Yield criteria and flow rules for porous ductile media", *J. Engg. Mats. Tech.*, **99** (1977), pp.2-15
26. V. Tvergaard, "On flow localisation in ductile materials containing spherical voids", *Int. J. Fracture*, **18** (1982), pp.237-252

27. V. Tvergaard and A. Needleman, "Analysis of the cup and cone fracture in a round tensile bar", *Acta Met.*, **32** (1984), pp.157-169

28. A. Saxena and L. Cretegny, "The relationship between microstructures and the J-R curve", *Met. & Mats. Trans.*, **29A** (1997), pp.1917-1922

29. R.H. Dodds and C.Ruggieri, "Modelling of constraint effects on ductile crack growth", Paper presented at the 27th National Symp. on Fatigue & Fracture, Williamsburg, VA, June 1995

30. R.O. Ritchie, J.F. Knott and J.R. Rice, "On the relationship between critical tensile stress and fracture toughness in mild steel", *J. Mech. Phys. Solids*, **21** (1973), pp.395-410

31. C.A. Hippsley and P. Bowen, "High temperature intergranular crack growth in martensitic 2.25 Cr-1 Mo steel", AERE Report R 12464, AERE Harwell, 1987

32. T.L. Anderson, "Fracture mechanisms in non-metals", in *Fracture Mechanics: Fundamentals and Applications*, CRC Press, USA, 1991, p.359

33. E399–90, "Standard test method for plane-strain fracture toughness of metallic materials", Annual Book of ASTM Standards, 1994, Vol.03.01, pp.407-437, ASTM, Philadelphia

34. E813–89, "Standard test method for J_{Ic}, a measure of fracture toughness", Annual Book of ASTM Standards, 1994, Vol.03.01, pp.628-642, ASTM, Philadelphia

35. E1290–93, "Standard test method for crack-tip opening displacement (CTOD) fracture toughness measurement", Annual Book of ASTM Standards, 1994, Vol.03.01, pp.846-855, ASTM, Philadelphia

36. E1737–96, "Standard test method for *J*-integral characterization of fracture toughness", Annual Book of ASTM Standards, 1996, Vol.03.01, pp.968-989, ASTM, Philadelphia

37. E647–93, "Standard test method for measurement of fatigue crack growth rates", Annual Book of ASTM Standards, 1994, Vol.03.01, pp.569-596, ASTM, Philadelphia

38. S.J.Hudak and R.J.Bucci (Eds.), "Fatigue crack growth measurement and data analysis", ASTM STP 738, ASTM, Pa., 1981

39. H.H.Johnson, "Calibrating the electric potential method for studying slow crack growth", *Mats. Res. & Standards*, **5** (1965), pp.442-445

40. A.Saxena and S.J.Hudak, Jr., "Review and extension of compliance information for common crack growth specimens", *Int. J. Fracture*, **14** (1978), pp.453-468

41. S.Tarafder, M.Tarafder and V.R.Ranganath, "Location independent CCL relations for standard fracture mechanics specimens" *Int J Fatigue*, **19** (1997), pp.635-640

42. S.Sivaprasad, S.Tarafder, M.Tarafder and K.K.Ray, "An alternative method for decreasing ΔK FCGR testing", *Int. J. Fatigue*, **22** (2000), pp.593-600

43. P. Paris and F. Erdogan, *J. Basic Eng.*, **85** (1963), p.528

44. PD 6493, "Guidelines on methods for assessing the acceptability of flaws in fusion welded structures", British Standard Institution, London, 1991

45. ASME-MPG-24, "Reference fracture toughness procedures applied to pressure vessel materials", American Society of Mechanical Engineers, 1984